

## Mass dependence of disappearance of transverse in-plane flow

Aman D. Sood and Rajeev K. Puri

*Physics Department, Panjab University, Chandigarh 160 014, India*

(Received 1 July 2003; revised manuscript received 20 January 2004; published 28 May 2004)

A theoretical study is presented for the disappearance of flow by analyzing a large number of reactions with masses between 47 and 476 units. We demonstrate that the effect of nucleon-nucleon cross sections reduces, to an insignificant level for heavier colliding nuclei in agreement with previous studies. A stiff equation of state with nucleon-nucleon cross sections  $\sigma=35\text{--}40$  mb is able to explain all the measured balance energies. A power law ( $\propto A^7$ ) is also given for the mass dependence of disappearance of flow, which is in good agreement with experimental data.

DOI: 10.1103/PhysRevC.69.054612

PACS number(s): 25.70.-z

### I. INTRODUCTION

The heavy-ion collisions at intermediate energies provide a rich physical insight into the reaction dynamics. One has measured (and/or predicted) several new phenomena that may shed light on the nature of hot and dense nuclear matter formed during a collision. In addition, one also hopes to understand the nature of nuclear interactions in medium. The prediction of collective transverse in-plane flow by the hydrodynamical model was a very important step towards understanding the excited nuclear matter [1]. The collective transverse in-plane flow was found to be very sensitive towards the different signals of excited nuclear matter. Apart from the transverse in-plane flow, one has also proposed, e.g., differential flow [2] and elliptic flow [3]. All these quantities are assumed to be sensitive towards (nuclear matter) equation of state and/or nucleon-nucleon ( $nn$ ) cross section, which is *the ultimate goal of the intermediate energy heavy-ion collisions*. One should, however, keep in mind that reaction dynamics depends also on the incident energy as well as on the impact parameter of the reaction. At low incident energies, dynamics is governed by the attractive mean field whereas repulsive interactions decide the fate of a reaction at higher incident energies. Naturally, the effect of  $nn$  collisions decreases with the decrease in incident energy. The dominance of the attractive mean field (at low incident energies) may prompt the emission of particles into backward hemisphere whereas if  $nn$  scatterings dominate, the particle emission is likely to be in the forward hemisphere. Therefore, while going from the low incident energy to higher energy, attractive interactions may be balanced by the repulsive interactions, resulting in the net zero flow (i.e., the disappearance of flow). The energy at which flow disappears is termed as balance energy [4].

During the last few years, extensive efforts have been made to measure and understand the disappearance of flow [5–17]. One has measured the balance energy  $E_{bal}$  in  $^{12}\text{C} + ^{12}\text{C}$  [5],  $^{20}\text{Ne} + ^{27}\text{Al}$  [5],  $^{36}\text{Ar} + ^{27}\text{Al}$  [7,17],  $^{40}\text{Ar} + ^{27}\text{Al}$  [8],  $^{40}\text{Ar} + ^{45}\text{Sc}$  [5,6,12],  $^{40}\text{Ar} + ^{51}\text{V}$  [9],  $^{64}\text{Zn} + ^{27}\text{Al}$  [10],  $^{40}\text{Ar} + ^{58}\text{Ni}$  [11],  $^{64}\text{Zn} + ^{48}\text{Ti}$  [17],  $^{58}\text{Ni} + ^{58}\text{Ni}$  [11–13],  $^{58}\text{Fe} + ^{58}\text{Fe}$  [13],  $^{64}\text{Zn} + ^{58}\text{Ni}$  [17],  $^{86}\text{Kr} + ^{93}\text{Nb}$  [5,12],  $^{93}\text{Nb} + ^{93}\text{Nb}$  [14],  $^{129}\text{Xe} + ^{118}\text{Sn}$  [11],  $^{139}\text{La} + ^{139}\text{La}$  [14], and  $^{197}\text{Au} + ^{197}\text{Au}$  [12,15,16] systems. The very recent and accurate measurement of the balance energy  $E_{bal}$  in  $^{197}\text{Au} + ^{197}\text{Au}$  [12,16] has

generated a renewed interest in the field [11]. Interestingly, most of the reported reactions are symmetric in nature. It should be kept in mind that the reaction dynamics depends also upon the asymmetry of the reaction [18]. All the above mentioned measurements were for the central collisions only. Some measurements [6,8,10–13], however, also took the impact parameter dependence into account. As noted in Ref. [12],  $E_{bal}$  for heavier nuclei shows little dependence on the impact parameter whereas a large variation in the  $E_{bal}$  can be seen for the lighter colliding nuclei [6,12]. The possible cause could be the fact that the disappearance of in-plane flow for heavier nuclei occurs at a much lower incident energy compared to lighter nuclei (e.g., the measured  $E_{bal}$  for  $^{197}\text{Au} + ^{197}\text{Au}$  is  $42 \pm 3 \pm 1$  MeV/nucleon [16] whereas it is  $111 \pm 10$  MeV/nucleon for  $^{20}\text{Ne} + ^{27}\text{Al}$  [5]). In the (near) absence of  $nn$  collisions at low incident energies, there should be a little dependence on the impact parameter [19]. Some attempts also exist in the literature where enhancement in the  $E_{bal}$  with neutron content was found experimentally and/or theoretically [13,20,21].

The above findings reveal the measurements of balance energy in more than 15 systems ranging from very light to heavy nuclei. As a result, a power law behavior ( $\propto A^7$ ) has also been reported for  $E_{bal}$  [5,12,16,17]. Earlier power law parameter  $\tau$  was supposed to be close to  $-1/3$  (resulting from the interplay between the attractive mean field and repulsive  $nn$  collisions) [5] whereas recent measurements suggest a deviation from the above mentioned power law [12,16].

Various theoretical attempts have been made to understand the vanishing of nuclear transverse in-plane flow. Most of these are, however, using the Boltzmann-Uehling-Uhlenbeck (BUU) model [2–5,8,10,12–14,16,21–26]. Some attempts are also reported in the literature where quantum molecular dynamics (QMD) model was used [6,20,27–31]. Different theoretical attempts considered either a stiff or soft equation of state along with a variety of  $nn$  cross sections. Interestingly, out of all these studies, only a couple of attempts exist where mass dependence of disappearance of flow was discussed [5,12,16,17,26,30,31]. A careful analysis shows that in Refs. [5,26] a total mass  $\leq 200$  was considered for the power law studies whereas in Refs. [30,31] only heavier masses  $\geq 175$  were analyzed. There  $E_{bal}$  for heavier

nuclei was found to scale approximately as  $1/\sqrt{A}$  [30,31] whereas lighter and medium mass nuclei follow  $A^{-1/3}$  dependence [5,26]. References [12,16] included for the first time a larger mass range  $63/47 \leq A \leq 394$ . However, even in these studies, only six systems were taken into account. (Note that power law fit was made for those systems which were recorded in the  $4\pi$  NSCL experiment. The data from the GANIL experiments, however, were not taken into account for fitting.)

The present aim is at least twofold.

(i) If one looks in the literature, one finds a lot of controversial findings with regard to the balance energy. One has often taken one reaction and tried to conclude about the nucleon-nucleon cross section. The conclusions, unfortunately, vary from author to author. For example, Ref. [8] reported a need of 41 mb cross section to explain the balance energy in Ar+Al system at  $b=3$  fm. Interestingly, there soft and hard equations of state gave the same balance energy. Contrarily, Li [25] has shown that a rather smaller cross section of 20 mb is needed to explain the balance energy in Ar+V. The cross section of 40 mb was overestimating the balance energy drastically. Zheng *et al.* [3] have shown that a soft equation of state with reduced cross section and a hard equation of state with normal cross section give the same balance energy for Ca-Ca reaction. On the other hand, balance energy was found to be sensitive to both hard and soft equations of state for Nb+Nb reaction [9]. The point to note here is that hard equation of state gives larger balance energy compared to soft equation of state. Zhou *et al.* [26] have shown that the hard and soft equations of state give same results over a wide range of masses. Contrary to these findings, Ref. [10] reported that a hard equation of state gives smaller balance energy in Zn+Al reactions compared to soft equation of state. From these examples, it is clear that a uniform study with one particular set of model parameters is missing. One would like to know whether it is possible to explain the balance energy over the whole range of masses with one set of parameter or not. This is important for extracting the magnitude of nucleon-nucleon cross section. In addition, one is also interested in investigating whether the same power law behavior can be extracted for the whole mass range or not.

(ii) We also aim to pin down the relative role of the mean field potential and nucleon-nucleon cross section in the disappearance of flow. It is argued that due to the counterbalancing of attractive and repulsive forces, the net transverse in-plane flow disappears.

The present study is carried out within the framework of the QMD model [18–20,27–34]. The details of the model are given in Sec. II. The results and discussion are presented in Sec. III and we summarize our results in Sec. IV.

## II. THE MODEL

We describe the time evolution of a heavy-ion reaction within the framework of QMD model [18–20,27–34] which is based on a molecular dynamics picture. Here each nucleon is represented by a coherent state of the form

$$\phi_\alpha(x_1, t) = \left( \frac{2}{L\pi} \right)^{3/4} e^{-[x_1 - x_\alpha(t)]^2} e^{ip_\alpha(x_1 - x_\alpha)} e^{-ip_\alpha^2 t/2m}. \quad (1)$$

Thus, the wave function has two time dependent parameters  $x_\alpha$  and  $p_\alpha$ . The total  $n$ -body wave function is assumed to be a direct product of coherent states:

$$\phi = \phi_\alpha(x_1, x_\alpha, p_\alpha, t) \phi_\beta(x_2, x_\beta, p_\beta, t) \dots, \quad (2)$$

where antisymmetrization is neglected. One should, however, keep in mind that the Pauli principle, which is very important at low incident energies, has been taken into account. The initial values of the parameters are chosen in a way that the ensemble  $(A_T + A_P)$  nucleons give a proper density distribution as well as a proper momentum distribution of the projectile and target nuclei. The time evolution of the system is calculated using the generalized variational principle. We start out from the action

$$S = \int_{t_1}^{t_2} \mathcal{L}[\phi, \phi^*] d\tau, \quad (3)$$

with the Lagrange functional

$$\mathcal{L} = \left( \phi \left| i\hbar \frac{d}{dt} - H \right| \phi \right), \quad (4)$$

where the total time derivative includes the derivatives with respect to the parameters. The time evolution is obtained by the requirement that the action is stationary under the allowed variation of the wave function:

$$\delta S = \delta \int_{t_1}^{t_2} \mathcal{L}[\phi, \phi^*] dt = 0. \quad (5)$$

If the true solution of the Schrödinger equation is contained in the restricted set of wave function  $\phi_\alpha(x_1, x_\alpha, p_\alpha)$ , this variation of the action gives the exact solution of the Schrödinger equation. If the parameter space is too restricted, we obtain that wave function in the restricted parameter space which comes close to the solution of the Schrödinger equation. Performing the variation with the test wave function (2), we obtain for each parameter  $\lambda$  an Euler-Lagrange equation

$$\frac{d}{dt} \frac{\partial \mathcal{L}}{\partial \dot{\lambda}} - \frac{\partial \mathcal{L}}{\partial \lambda} = 0. \quad (6)$$

For each coherent state and a Hamiltonian of the form  $H = \sum_\alpha [T_\alpha + \frac{1}{2} \sum_{\alpha\beta} V_{\alpha\beta}]$ , the Lagrangian and the Euler-Lagrange function can be easily calculated [33]:

$$\mathcal{L} = \sum_\alpha \dot{\mathbf{x}}_\alpha \cdot \mathbf{p}_\alpha - \sum_\beta \langle V_{\alpha\beta} \rangle - \frac{3}{2Lm}, \quad (7)$$

$$\dot{\mathbf{x}}_\alpha = \frac{\mathbf{p}_\alpha}{m} + \nabla_{p_\alpha} \sum_\beta \langle V_{\alpha\beta} \rangle, \quad (8)$$

$$\dot{\mathbf{p}}_\alpha = -\nabla_{\mathbf{x}} \sum_{\beta} \langle V_{\alpha\beta} \rangle. \quad (9)$$

Thus, the variational approach has reduced the  $n$ -body Schrödinger equation to a set of  $6n$  different equations for the parameters which can be solved numerically. If one inspects the formalism carefully, one finds that the interaction potential which is actually the Bruckner  $G$  matrix can be divided into two parts: (i) a real part and (ii) an imaginary part. The real part of the potential acts like a potential whereas the imaginary part is proportional to the cross section.

In the present model, interaction potential comprises the following terms:

$$V_{\alpha\beta} = V_{loc}^2 + V_{loc}^3 + V_{Coul} + V_{Yuk}, \quad (10)$$

$V_{loc}$  is the Skyrme force whereas  $V_{Coul}$  and  $V_{Yuk}$  define, respectively, the Coulomb and Yukawa terms. The expectation values of these potentials are calculated as

$$V_{loc}^2 = \int f_\alpha(\mathbf{p}_\alpha, \mathbf{r}_\alpha, t) f_\beta(\mathbf{p}_\beta, \mathbf{r}_\beta, t) V_I^{(2)}(\mathbf{r}_\alpha, \mathbf{r}_\beta) \times d^3\mathbf{r}_\alpha d^3\mathbf{r}_\beta d^3\mathbf{p}_\alpha d^3\mathbf{p}_\beta, \quad (11)$$

$$V_{loc}^3 = \int f_\alpha(\mathbf{p}_\alpha, \mathbf{r}_\alpha, t) f_\beta(\mathbf{p}_\beta, \mathbf{r}_\beta, t) f_\gamma(\mathbf{p}_\gamma, \mathbf{r}_\gamma, t) \times V_I^{(3)}(\mathbf{r}_\alpha, \mathbf{r}_\beta, \mathbf{r}_\gamma) d^3\mathbf{r}_\alpha d^3\mathbf{r}_\beta d^3\mathbf{r}_\gamma d^3\mathbf{p}_\alpha d^3\mathbf{p}_\beta d^3\mathbf{p}_\gamma \quad (12)$$

where  $f_\alpha(\mathbf{p}_\alpha, \mathbf{r}_\alpha, t)$  is the Wigner density which corresponds to the wave functions [Eq. (2)]. If we deal with the local Skyrme force only, we get

$$V^{Skyrme} = \sum_{\alpha=1}^{A_T+A_P} \left[ \frac{A}{2} \sum_{\beta=1} \left( \frac{\tilde{\rho}_{\alpha\beta}}{\rho_0} \right) + \frac{B}{C+1} \sum_{\beta \neq \alpha} \left( \frac{\tilde{\rho}_{\alpha\beta}}{\rho_0} \right)^C \right]. \quad (13)$$

Here  $A$ ,  $B$ , and  $C$  are the Skyrme parameters which are defined according to the ground state properties of a nucleus. Different values of  $C$  lead to different equations of state. A larger value of  $C$  ( $=380$  MeV) is often dubbed as stiff equation of state.

A number of attempts exist in the literature which study the nature of equation of state. Following Refs. [2–4,6,8,10,22,24,26–31], we shall also employ a stiff equation of state throughout the present analysis. It should also be noted that the success rate is nearly the same for stiff and soft equations of state. Further, it has been shown in Refs. [8,10,22,24,26] that the difference between  $E_{bal}$  using a stiff and soft equation of state is insignificant for central heavy-ion collisions.

The imaginary part of the potential, i.e., the  $nn$  cross section, has been a point of controversy. A large number of calculations exist where a constant and isotropic cross section has been used. Following Refs. [8,10,22,24,29–31,35,36], we also use a constant energy independent cross section. As shown by Li [25], most of the

collisions below 100 MeV/nucleon happen with  $nn$  cross section of 55 mb strength. Keeping the present energy domain in mind, the choice of a constant cross section is justified. It has also been shown by Zheng *et al.* [3] that a stiff equation of state with free  $nn$  cross section and a soft equation of state with reduced cross section yield nearly the same results. For comparison, we shall also use an energy dependent cross section as fitted by Cugnon [33] (labeled as Cug) as well as a medium dependent cross section derived from  $G$  matrix [33] (denoted by GMC). As shown by Li *et al.* [21], the isospin degree of freedom in nucleon-nucleon cross section is not important for central collisions as in the present case. The role of isospin dependent cross section is, however, significant once one shifts to peripheral collisions.

### III. RESULTS AND DISCUSSION

Using a stiff equation of state along with different  $nn$  cross sections, we simulated the above mentioned reactions for 1000–3000 events in each case. The reactions were followed till transverse in-plane flow saturates. The saturation time varies between 150 fm/c (for lighter colliding nuclei such as  $^{20}\text{Ne} + ^{27}\text{Al}$ ) and 300 fm/c (for heavier colliding nuclei such as  $^{197}\text{Au} + ^{197}\text{Au}$ ). In particular, for the present mass dependent analysis, we simulated the reactions of  $^{20}\text{Ne} + ^{27}\text{Al}$  ( $b/b_{max}=0.4$ ),  $^{36}\text{Ar} + ^{27}\text{Al}$  ( $b=2.5$  fm),  $^{40}\text{Ar} + ^{27}\text{Al}$  ( $b=1.6$  fm),  $^{40}\text{Ar} + ^{45}\text{Sc}$  ( $b/b_{max}=0.4$ ),  $^{40}\text{Ar} + ^{51}\text{V}$  ( $b/b_{max}=0.3$ ),  $^{40}\text{Ar} + ^{58}\text{Ni}$  ( $b=0-3$  fm),  $^{64}\text{Zn} + ^{48}\text{Ti}$  ( $b=2$  fm),  $^{58}\text{Ni} + ^{58}\text{Ni}$  ( $b/b_{max}=0.28$ ),  $^{64}\text{Zn} + ^{58}\text{Ni}$  ( $b=2$  fm),  $^{86}\text{Kr} + ^{93}\text{Nb}$  ( $b/b_{max}=0.4$ ),  $^{93}\text{Nb} + ^{93}\text{Nb}$  ( $b/b_{max}=0.3$ ),  $^{129}\text{Xe} + ^{\text{nat}}\text{Sn}$  ( $b=0-3$  fm),  $^{139}\text{La} + ^{139}\text{La}$  ( $b/b_{max}=0.3$ ), and  $^{197}\text{Au} + ^{197}\text{Au}$  ( $b=2.5$  fm). Since our present interest is to study the experimentally measured balance energies, the choice of impact parameter is guided by the experimentally extracted information [5–17]. In experiments, one often takes scaled impact parameters. The corresponding theoretical attempts also used the scaled impact parameter. The above reactions were simulated at incident energies between 30 MeV/nucleon and 150 MeV/nucleon depending upon the mass of the system. Naturally, a lower energy range was used for heavy nuclei whereas a higher beam energy was needed for lighter cases. The reactions were simulated at different fixed incident energies and a straight line interpolation was used to find the balance energy  $E_{bal}$ .

There are several methods used in the literature to define the nuclear transverse in-plane flow. In most of the studies, balance energy is extracted from  $(p_x/A)$  plots where one plots  $(p_x/A)$  as a function of  $Y_{c.m.}/Y_{beam}$ . Using a linear fit to the slope, one can define the so-called reduced flow  $F$ . Naturally, the energy at which reduced flow passes through zero is called the balance energy. Alternatively, one can also use a more integrated quantity “directed transverse in-plane flow  $\langle p_x^{dir} \rangle$ ” which is defined as [28–34]

$$\langle p_x^{dir} \rangle = \frac{1}{A} \sum_i \text{sgn}\{Y(i)\} p_x(i), \quad (14)$$

where  $Y(i)$  and  $p_x(i)$  are the rapidity distribution and transverse momentum of the  $i$ th particle. In this definition, all

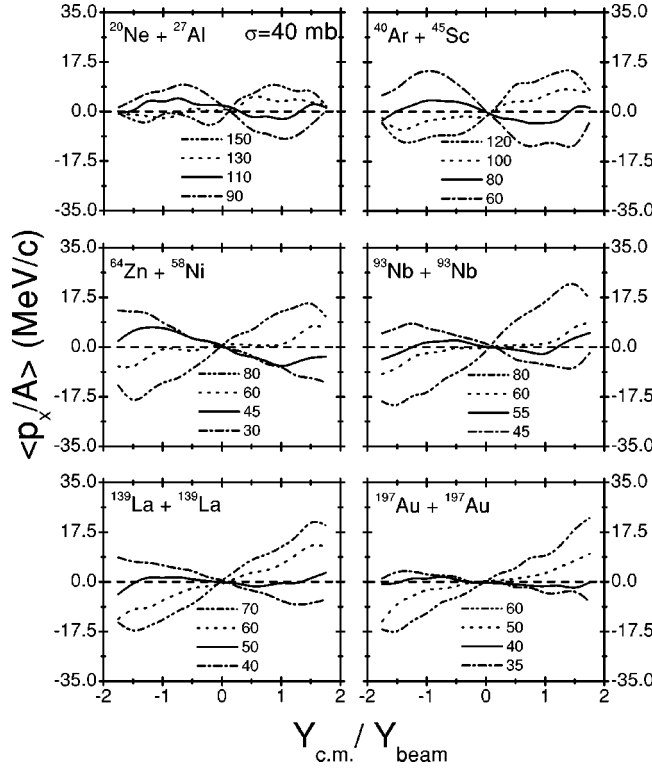


FIG. 1. The averaged  $\langle p_x/A \rangle$  as a function of  $Y_{c.m.}/Y_{beam}$ . Here we display the results at different incident energies using a stiff equation of state along with  $\sigma=40$  mb. The reactions of  $^{20}\text{Ne} + ^{27}\text{Al}$  and  $^{40}\text{Ar} + ^{45}\text{Sc}$  are at 150 fm/c whereas those of  $^{64}\text{Zn} + ^{58}\text{Ni}$ ,  $^{93}\text{Nb} + ^{93}\text{Nb}$ ,  $^{139}\text{La} + ^{139}\text{La}$  and  $^{197}\text{Au} + ^{197}\text{Au}$  are at 300 fm/c.

rapidity bins are taken into account. It, therefore, presents an easier way of measuring the in-plane flow rather than complicated functions such as  $(p_x/A)$  plots. It is worth mentioning that the balance energy is independent of the nature of the emitted particle [5]. Further, the apparatus corrections and acceptance do not play any role in calculating the energy of vanishing flow [5,9].

In Fig. 1, we display the final state transverse momentum  $\langle p_x/A \rangle$  as a function of rapidity, which is defined as

$$Y(i) = \frac{1}{2} \ln \frac{\mathbf{E}(i) + \mathbf{p}_z(i)}{\mathbf{E}(i) - \mathbf{p}_z(i)}, \quad (15)$$

where  $\mathbf{E}(i)$  and  $\mathbf{p}_z(i)$  are, respectively, the total energy and longitudinal momentum of the  $i$ th particle. The upper parts are for  $^{20}\text{Ne} + ^{27}\text{Al}$  (at 150 fm/c) and  $^{40}\text{Ar} + ^{45}\text{Sc}$  (at 150 fm/c), whereas the bottom parts are for  $^{139}\text{La} + ^{139}\text{La}$  (at 300 fm/c) and  $^{197}\text{Au} + ^{197}\text{Au}$  (at 300 fm/c). The middle parts are for  $^{64}\text{Zn} + ^{58}\text{Ni}$  (at 300 fm/c) and  $^{93}\text{Nb} + ^{93}\text{Nb}$  (at 300 fm/c). In all the cases, the slope is negative at lower incident energies which changes to positive value at higher incident energies. Between these limits, the slope becomes almost zero at a particular energy. This zero slope energy is termed as balance energy. One also notices that a higher incident energy is needed in lighter cases to balance the at-

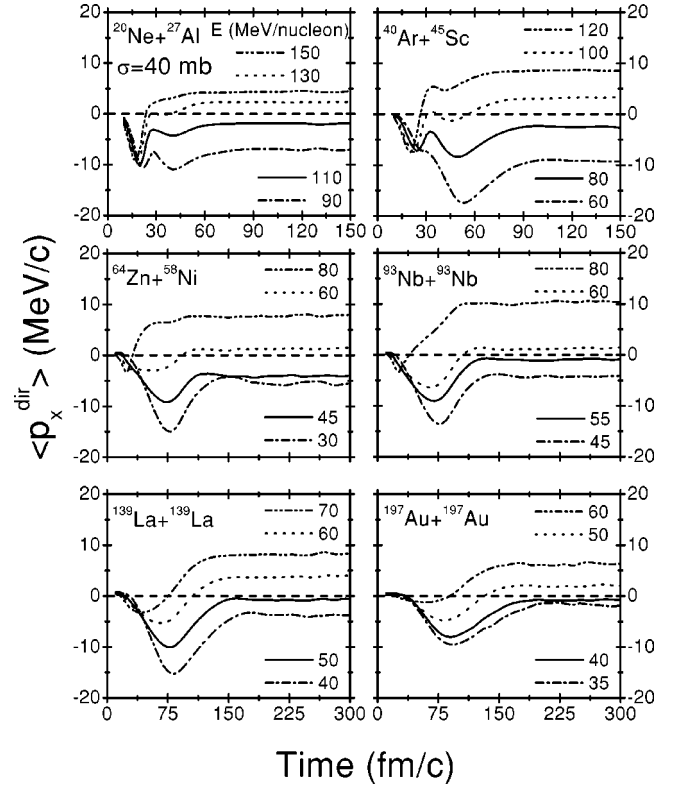


FIG. 2. The time evolution of  $\langle p_x^{dir} \rangle$  as a function of time. Here again results are for stiff equation of state along with  $\sigma=40$  mb.

tractive and repulsive forces. This energy decreases with increase in the mass of the system.

A look at Fig. 2, where  $\langle p_x^{dir} \rangle$  (instead of  $\langle p_x/A \rangle$ ) is plotted, depicts quite similar trends. Here  $\langle p_x^{dir} \rangle$  is displayed as a function of reaction time. The  $\langle p_x^{dir} \rangle$  is always negative during initial phase of the reaction irrespective of the incident energy. This shows that the interactions among nuclei are attractive during initial phase of the reaction. These interactions remain either attractive throughout the time evolution or may turn repulsive depending on the incident energy. The transverse in-plane flow in lighter colliding nuclei saturates earlier compared to heavy colliding nuclei. One also sees a sharp transition from negative to positive flow in lighter nuclei. This transition is gradual when one analyzes the heavier nuclei. If one compares Figs. 1 and 2, one finds that the disappearance of flow (where flow is zero) occurs at the same incident energies in both cases showing the equivalence between  $(p_x/A)$  and  $\langle p_x^{dir} \rangle$  as far as balance energy is concerned. The latter quantity is more useful since it is more stable than the former one. These findings are in agreement with Refs. [28,29].

It has been advocated by several authors that the study of disappearance of flow can shed light on the magnitude of  $nn$  cross section [3,5,8,10,12,13,16,22,24–26,28–31]. To check this point with reference to mass dependence, we show in Fig. 3, the final stage  $\langle p_x^{dir} \rangle$  as a function of incident energy. The left top, middle, and bottom panels are for  $^{20}\text{Ne} + ^{27}\text{Al}$ ,  $^{64}\text{Zn} + ^{58}\text{Ni}$ , and  $^{139}\text{La} + ^{139}\text{La}$ , respectively, whereas top, middle, and bottom panels on the right-hand side display the results of, respectively,  $^{40}\text{Ar} + ^{45}\text{Sc}$ ,  $^{93}\text{Nb} + ^{93}\text{Nb}$ , and  $^{197}\text{Au}$

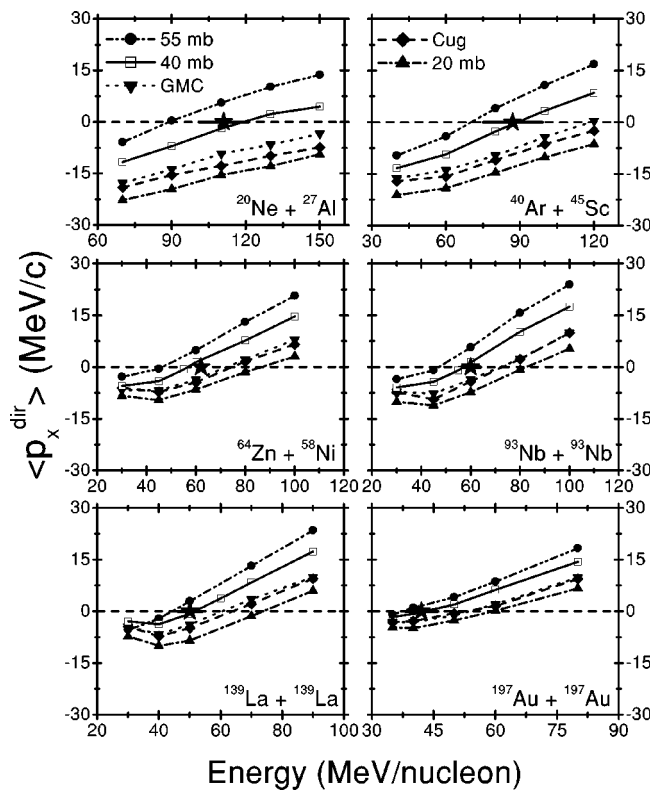


FIG. 3.  $\langle p_x^{dir} \rangle$  as a function of incident energy. The results for different cross sections of 55, 40, and GMC are represented, respectively, by the solid circles, open squares, and solid inverted triangles whereas for Cug and 20 mb results are represented by solid diamonds and solid triangles. A stiff equation of state has been used. All lines are to guide the eyes.

+ $^{197}\text{Au}$ . The experimental data are displayed by stars whereas our present results with  $\sigma=55$ , 40, and 20 mb are shown, respectively, by solid circles, open squares, and solid triangles. The  $\langle p_x^{dir} \rangle$  obtained with energy dependent cross section due to Cugnon (labeled as Cug) and the one that takes the medium into account (i.e., the  $G$  matrix) are marked by solid diamonds and inverted triangles, respectively. First of all, we see that the medium effects in  $nn$  cross section do not play any role at these low incident energies. The results obtained with the Cugnon energy dependent cross section and  $G$ -matrix medium dependent cross section are roughly the same for heavier colliding nuclei. Some visible differences, however, can be seen in the case of light colliding nuclei where incident energy is relatively high. Further, energy dependent cross section due to Cugnon and a constant cross section of 20 mb strength give quite close results, which is in agreement with the finding of Ref. [25]. One also sees a linear enhancement in the nuclear flow with increase in the incident energy. Further, the role of different cross sections is consistent throughout the present mass range. The largest cross section gives more positive flow which is followed by the second largest cross section. Interestingly, these effects depend on the mass of the system. If one looks at the reaction of  $^{20}\text{Ne} + ^{27}\text{Al}$ , one sees that the  $E_{bal}$  increases from 89 MeV/nucleon to 244 MeV/nucleon when  $nn$  cross sections are reduced from 55 mb to 20 mb, whereas

the range of  $E_{bal}$  for the same cross sections was 47–83 MeV/nucleon for  $^{93}\text{Nb} + ^{93}\text{Nb}$  reaction. If one goes to still heavier nuclei,  $^{197}\text{Au} + ^{197}\text{Au}$ , the range of  $E_{bal}$  narrows down to 38–59 MeV/nucleon. In other words, a reduction in the cross section by 64% yields a change of 155 MeV/nucleon in the case of  $^{20}\text{Ne} + ^{27}\text{Al}$  reaction, whereas it is only 21 MeV/nucleon for the case of  $^{197}\text{Au} + ^{197}\text{Au}$ . Similarly looking at the curves of  $\sigma=55$  and 40 mb, a reduction in the cross section by 27% yields a difference of 30 MeV/nucleon in the  $E_{bal}$  for  $^{20}\text{Ne} + ^{27}\text{Al}$  reaction whereas nearly 4 MeV/nucleon difference exists for the case of  $^{197}\text{Au} + ^{197}\text{Au}$  reaction. This result, which is in agreement with the findings of Refs. [12,13], depicts that for heavier colliding nuclei,  $E_{bal}$  is independent of the cross section one is choosing. Further, the standard energy dependent  $nn$  cross section (Cug) fails to reproduce the observed balance energy in almost all the cases. However, a constant cross section of 40 mb strength seems to be closer to the experimentally observed balance energy. This conclusion is supported by several other groups where a cross section of 30–40 mb was reported to reproduce the experimental data [8,10,22,24–26,29–31,35,36]. This will be discussed further in detail in the following paragraphs.

It has been argued in Refs. [28,37] that the flow at any point during the reaction can be divided into the parts emerging from the (attractive) mean field potential and (repulsive)  $nn$  collision contributions. Following Ref. [28], we decomposed the transverse momentum into the contributions created by the mean field and two-body  $nn$  collisions. This extraction, which is made from the simulations of the QMD model, is done as following [28]: Here at each time step during the collision, momentum transferred by the mean field and two-body collision is analyzed separately. Naturally, we get two values at each time step which can be followed throughout the reaction. The total transverse momentum can be obtained by adding both these contributions.

In Fig. 4, we display the final state  $\langle p_x^{dir} \rangle$  decomposed into two parts, i.e., into the mean field and two-body collision parts as a function of the incident energies for different colliding systems as reported in Fig. 3. Again a linear enhancement in the flow with incident energy can be seen. Further, the contribution of the mean field remains attractive throughout the energy range whereas collision contribution is always repulsive. The balancing of both these contributions results in net zero flow. One should, however, keep in mind that the contribution of the mean field potential may even turn repulsive at higher incident energies [37].

In Fig. 5, we display the energy of vanishing flow ( $E_{bal}$ ) as a function of combined mass of the system that ranges from  $^{20}\text{Ne} + ^{27}\text{Al}$  to  $^{197}\text{Au} + ^{197}\text{Au}$ . In our earlier communication [31], a prediction of  $E_{bal}$  for  $^{238}\text{U} + ^{238}\text{U}$  was also made. Apart from the experimental data, we also show our results for  $\sigma=35$  and 40 mb. All curves are a fit of the form  $cA^\tau$  using  $\chi^2$  minimization procedure. The experimental data can be fitted by  $\tau_{expt} = -0.42 \pm 0.05$  whereas our present results with  $\sigma=40$  mb has  $\tau_{40} = -0.42 \pm 0.08$ . The results with  $\sigma=35$  mb yield  $\tau_{35} = -0.43 \pm 0.09$ . Exclusively, one can extract the following.

(1) The present value of  $\tau_{expt}$  differs from the earlier reported results ( $\tau_{expt} = -1/3$  for  $A \leq 200$  [5] and  $\tau_{expt} =$

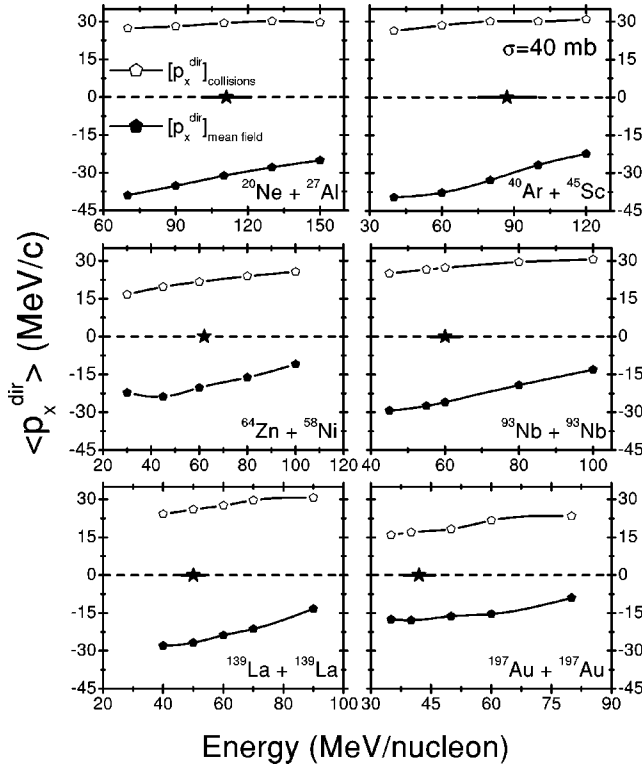


FIG. 4. The decomposition of  $\langle p_x^{dir} \rangle$  into collision and mean field parts as a function of incident beam energy. Here results are displayed for  $\sigma=40$  mb. Stars are the experimental balance energy.

$-0.46 \pm 0.06$  [16] for  $A \leq 400$  mass). Note that in earlier attempts [12,16], the data of NSCL alone were used to fit the power law.

(2) The present theoretical value  $\tau_{40} = -0.42 \pm 0.08$  is the closest one obtained so far. In earlier reports [5],  $\tau_{expt}$  was

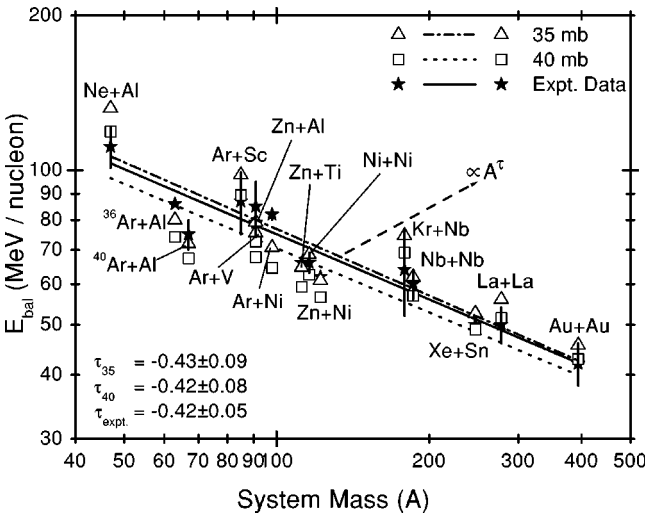


FIG. 5. Balance energy as a function of combined mass of the system. The experimental points along with error bars are displayed by solid stars whereas our theoretical calculations for  $\sigma=35$  and 40 mb are shown by open triangles and squares. The lines are the power law  $\propto cA^\tau$ . The solid, dashed, and dash-dotted lines represent the power law fit for experimental points, with  $\sigma=40$  and 35 mb, respectively.

$-1/3$  whereas BUU model yielded  $-0.28 \leq \tau_{th} \leq -0.32$ . In another study [16], the  $\tau_{expt}$  was  $-0.46 \pm 0.06$  whereas BUU model has  $\tau_{th} = -0.41 \pm 0.03$ . In other words, the present QMD model with a stiff equation of state along with  $\sigma = 35-40$  mb can explain the data much better than any other theoretical calculations. In addition, our present analysis has much wider mass spectrum than any early attempt. Some visible deviations in the middle order are also reported by other authors [25].  $\sigma=40$  mb explains  $E_{bal}$  in heavier nuclei whereas  $\sigma=35$  mb reproduces middle order nicely. Some fluctuations are also due to the asymmetry of the colliding nuclei that will not follow the power law of symmetric nuclei at the first place.

(3) From the figure, it is also evident that a true cross section for this energy domain should be between 35 and 40 mb. This conclusion is very important since a wide range of masses was used for the present analysis. Our conclusion about the strength of  $nn$  cross section is in agreement with large number of earlier calculations on disappearance of flow and other phenomena in heavy-ion collisions [8,10,22,24-26,29-31,35,36]. As noted in Ref. [26], this value of  $nn$  cross section is still much smaller than the actual averaged free  $nn$  cross section, which is about 60 mb [38]. In case of fragmentation, a larger cross section of  $\sigma=55$  mb is also suggested [35].

We have also tried to fit the balance energy in terms of other parameters such as the charge of colliding nuclei. This attempt is shown in Fig. 6 where  $E_{bal}$  is plotted as a function of the total atomic number of the system. In the upper part, we display the full range of systems whereas in the lower part, only heavier nuclei are taken into picture. A power law  $\propto Z^\tau$  fits the data nicely. Now  $\tau$  is  $-0.47 \pm 0.05$  ( $-0.46 \pm 0.09$ ) for experimental data (theoretical results) which is larger compared to mass power law [ $\tau = -0.42 \pm 0.05$  ( $-0.42 \pm 0.08$ )] for experiment data (theoretical results). This difference in the slopes stems from a different charge to mass ratio in lighter and heavy nuclei. Interestingly, the value of  $\tau$  for heavier nuclei [see Fig. 6(b)] is  $-0.59 \pm 0.06$  ( $-0.58 \pm 0.11$ ). This result, which is in agreement with Ref. [16], shows the dominance of the Coulomb interactions in heavier colliding nuclei. It would be of further interest to investigate whether the flow due to the collision and mean field parts (at the balance energy) exhibit any mass dependence or not. We display, in Fig. 7, the flow  $\langle p_x^{dir} \rangle$  at balance energy due to collision (upper) and mean field parts (lower). Interestingly, we do not see any clear mass dependence. Rather very weak dependence (with  $\tau = -0.09 \pm 0.08$ ) exists on the system size. This is in agreement with Ref. [37], where a similar conclusion was drawn.

IV. SUMMARY

We have studied the mass dependence of the disappearance of flow in a large number of colliding nuclei using QMD model. A large number of reactions with masses between 47 and 476 were studied where experimental balance energy is available. Our findings suggest a weak dependence of different cross sections for heavier colliding nuclei in agreement with Ref. [12]. Our calculations with a stiff equa-

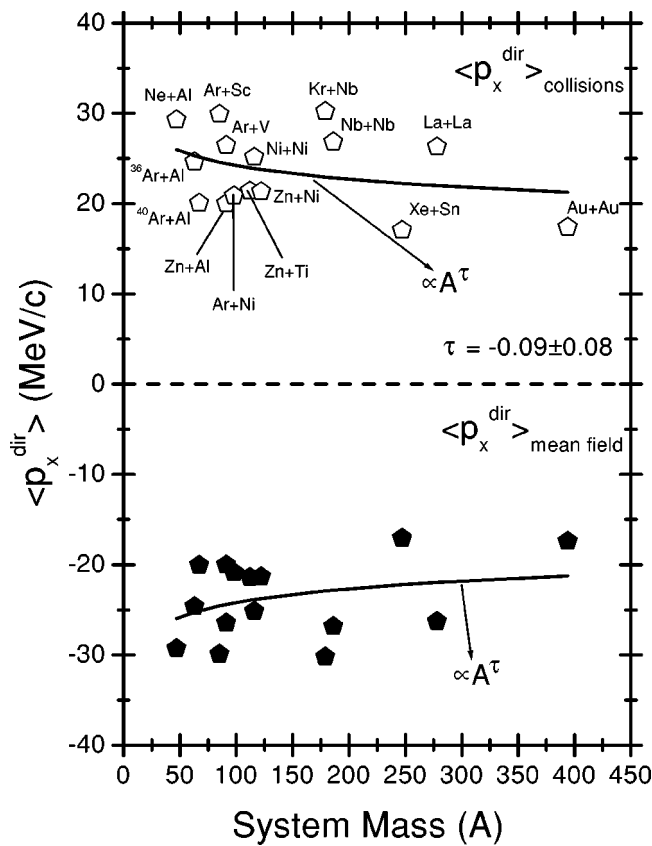


FIG. 7. The decomposition of the  $\langle p_x^{dir} \rangle$  at balance energy into collision and mean field parts. The results are obtained using a stiff equation of state along with  $\sigma=40$  mb.

tion of state are in good agreement with experimental data. We could also reproduce the slope of the power law ( $\propto A^\tau$ ) over a wide range of masses. Our calculations suggest a cross section of 35–40 mb in this incident energy domain. We also showed that the collective flow due to mean field is attractive whereas it is repulsive for collision part. The balancing of these two parts results in the disappearance of flow.

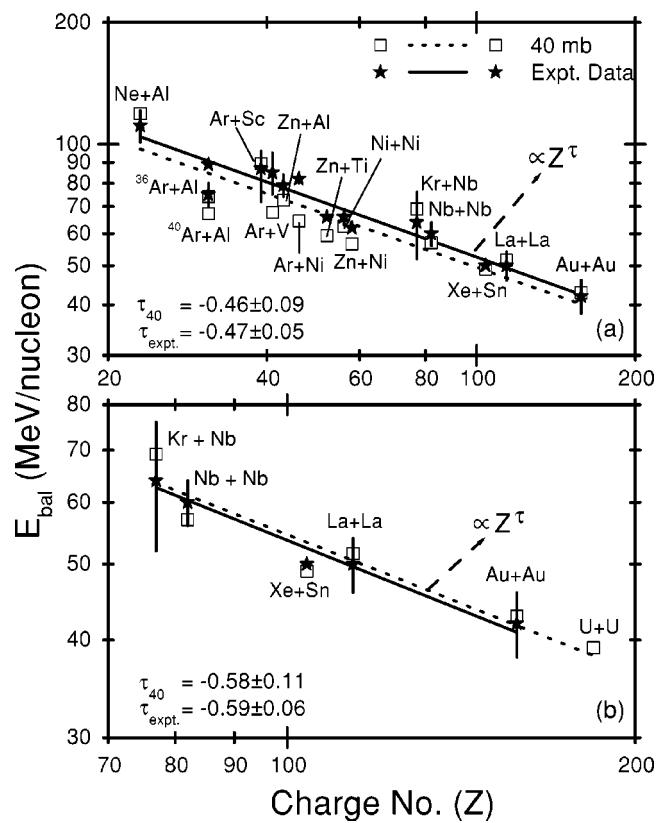


FIG. 6. (a) Balance energy as a function of atomic number  $Z$ . Here we display the experimental results along with our calculations for  $\sigma=40$  mb. The fits are obtained with  $\chi^2$  minimization for power law function  $cZ^\tau$ . (b) Same as (a), but for heavier nuclei.

#### ACKNOWLEDGMENT

This work was supported by the grant (Grant No. SP/S2/K-21/96) from Department of Science and Technology, Government of India.

- [1] W. Scheid, H. Müller, and W. Greiner, Phys. Rev. Lett. **32**, 741 (1974).
- [2] B. A. Li and A. T. Sustich, Phys. Rev. Lett. **82**, 5004 (1999).
- [3] Y. M. Zheng, C. M. Ko, B. A. Li, and B. Zhang, Phys. Rev. Lett. **83**, 2534 (1999).
- [4] J. J. Molitoris and H. Stöcker, Phys. Lett. **162B**, 47 (1985); V. de la Mota, F. Sebille, M. Farine, B. Remaud, and P. Schuck, Phys. Rev. C **46**, 677 (1992); G. F. Bertsch, W. G. Lynch, and M. B. Tsang, Phys. Lett. B **189**, 384 (1987); D. Krofcheck *et al.*, Phys. Rev. Lett. **63**, 2028 (1989).
- [5] G. D. Westfall *et al.*, Phys. Rev. Lett. **71**, 1986 (1993).
- [6] R. Pak, O. Bjarki, S. A. Hannuschke, R. A. Lacey, J. Lauret, W. J. Llope, A. Nadasen, N. T.B. Stone, A. M. Vander Molen, and G. D. Westfall, Phys. Rev. C **54**, 2457 (1996); R. Pak *et al.*, *ibid.* **53**, R1469 (1996).
- [7] J. C. Angeliqne *et al.*, Nucl. Phys. **A614**, 261 (1997).
- [8] J. P. Sullivan *et al.*, Phys. Lett. B **249**, 8 (1990).
- [9] D. Krofcheck *et al.*, Phys. Rev. C **43**, 350 (1991); C. A. Ogilvie *et al.*, *ibid.* **42**, R10 (1990).
- [10] Z. Y. He *et al.*, Nucl. Phys. **A598**, 248 (1996).
- [11] D. Cussol *et al.*, Phys. Rev. C **65**, 044604 (2002).
- [12] D. J. Magestro, W. Bauer, and G. D. Westfall, Phys. Rev. C **62**, 041603(R) (2000).
- [13] G. D. Westfall, Nucl. Phys. **A681**, 343c (2001); R. Pak *et al.*, Phys. Rev. Lett. **78**, 1026 (1997); **78**, 1022 (1997).
- [14] D. Krofcheck *et al.*, Phys. Rev. C **46**, 1416 (1992).
- [15] W. M. Zhang *et al.*, Phys. Rev. C **42**, R491 (1990); M. D. Partlan *et al.*, Phys. Rev. Lett. **75**, 2100 (1995); P. Crochet *et al.*, Nucl. Phys. **A624**, 755 (1997).
- [16] D. J. Magestro, W. Bauer, O. Bjarki, J. D. Crispin, M. L. Miller, M. B. Tonjes, A. M. Vander Molen, G. D. Westfall, R. Pak, and E. Norbeck, Phys. Rev. C **61**, 021602(R) (2000).

- [17] A. Buta *et al.*, Nucl. Phys. **A584**, 397 (1995).
- [18] J. Singh, S. Kumar, and R. K. Puri, Phys. Rev. C **62**, 044617 (2000).
- [19] R. K. Puri and S. Kumar, Phys. Rev. C **57**, 2744 (1998); Zhuxia Li, C. Hartnack, H. Stöcker, and W. Greiner, *ibid.* **44**, 824 (1991).
- [20] C. Liewen, Z. Fengshou, and J. Genming, Phys. Rev. C **58**, 2283 (1998).
- [21] B. A. Li, Z. Ren, C. M. Ko, and S. J. Yennello, Phys. Rev. Lett. **76**, 4492 (1996).
- [22] H. Zhou, Z. Li, Y. Zhuo, and G. Mao, Nucl. Phys. **A580**, 627 (1994).
- [23] D. Klakow, G. Welke, and W. Bauer, Phys. Rev. C **48**, 1982 (1993).
- [24] H. M. Xu, *et al.*, Phys. Rev. C **46**, R389 (1992); H. M. Xu, Phys. Rev. Lett. **67**, 2769 (1991).
- [25] B. A. Li, Phys. Rev. C **48**, 2415 (1993).
- [26] H. Zhou, Z. Li, and Y. Zhuo, Phys. Rev. C **50**, R2664 (1994).
- [27] S. Soff, S. A. Bass, C. Hartnack, H. Stöcker, and W. Greiner, Phys. Rev. C **51**, 3320 (1995).
- [28] E. Lehmann, A. Faessler, J. Zipprich, R. K. Puri, and S. W. Huang, Z. Phys. A **355**, 55 (1996).
- [29] S. Kumar, M. K. Sharma, R. K. Puri, K. P. Singh, and I. M. Govil, Phys. Rev. C **58**, 3494 (1998).
- [30] A. Sood and R. K. Puri, Symposium on Nuclear Physics, 2002, Vol. 45B, p. 288; A. Sood and R. K. Puri, Proceedings of the VIII International Conference on Nucleus-Nucleus Collisions, Moscow, Russia, 2003 (unpublished).
- [31] A. D. Sood, R. K. Puri, and J. Aichelin, Phys. Lett. B (submitted).
- [32] S. Kumar, R. K. Puri, and J. Aichelin, Phys. Rev. C **58**, 1618 (1998).
- [33] J. Aichelin, Phys. Rep. **202**, 233 (1991); J. Aichelin and H. Stöcker, Phys. Lett. B **176**, 14 (1986).
- [34] C. Hartnack, R. K. Puri, J. Aichelin, J. Konopka, S. A. Bass, H. Stöcker, and W. Greiner, Eur. Phys. J. A **1**, 151 (1998).
- [35] H. W. Barz, J. P. Bondorf, D. Idier, and I. N. Mishustin, Phys. Lett. B **382**, 343 (1996).
- [36] C. Roy *et al.*, Z. Phys. A **358**, 73 (1997).
- [37] B. Blättel, V. Koch, A. Lang, K. Weber, W. Cassing, and U. Mosel, Phys. Rev. C **43**, 2728 (1991).
- [38] K. Chen, Z. Fraenkel, G. Friedlander, J. R. Grover, J. M. Miller, and Y. Shimamoto, Phys. Rev. **166**, 949 (1968).